

Molecular Dynamics Simulations of Gas Diffusion in Metal–Organic Frameworks: Argon in CuBTC

Anastasios I. Skoulidas*

NETL Research Associate, U.S. Department of Energy, National Energy and Technology Laboratory,
P.O. Box 10940, Pittsburgh, Pennsylvania 15236-0940

Received October 24, 2003; E-mail: anastasios.skoulidas@netl.doe.gov

The class of coordination polymers known as metal–organic frameworks (MOFs) has three-dimensional porous structures that are considered as a promising alternative to zeolites and other nanoporous materials for catalysis, adsorption, and separation applications. MOFs based on metal-oxide building blocks linked together with organic molecules have very stable structures with high porosity.^{1–3} Considering the rich coordination chemistry of transition metals and the many possibilities of different organic molecules acting as bridges, MOFs offer an avenue for creating designer nanoporous materials.³

Experimental studies of adsorption in MOFs^{1,2,5–10} as well as recent computational studies by Vishnyakov et al.¹⁰ have shown that MOFs have open networks with large pore volumes and hence larger adsorption capacities. Nevertheless, their adsorptive properties are qualitatively similar to those of zeolites.

A question arises about how the larger and more open structures of MOFs and their unique chemical composition might affect the diffusion of molecules through them and, therefore, limit or broaden their possible practical applications. To address this issue, simulation techniques that have been used previously to study transport of light gases in zeolites^{11–14} have been employed to examine Ar diffusion in copper(II) benzene-1,3,5-tricarboxylate metal–organic framework (CuBTC). These methods are known to give results in quantitative agreement with experiments for gas diffusion in silicalite.^{12,13} This paper presents the first study of gas diffusion inside an MOF and compares the observed diffusion to known behaviors in zeolites.

The diffusion of a single adsorbed species can be characterized by two distinct diffusivities.^{4,15–18} The self-diffusivity, $D_s(c)$ measures the displacement of a tagged molecule as it diffuses at equilibrium inside a crystal, at a specified concentration c . Macroscopic diffusion of a single adsorbed species in a crystal can be characterized by using the transport diffusivity, $D_t(c)$, which is defined as the proportionality constant relating a macroscopic flux, J , to a macroscopic concentration gradient: $J = -D_t(c)\nabla c$. $D_t(c)$ is often written as $D_t(c) = D_0(c)\Gamma$. $D_0(c)$ is the corrected diffusivity, and Γ is the thermodynamic correction factor.^{11–14} D_0 is more closely related to the dynamics of the system than is D_t .¹⁵ Previous studies have shown that these quantities can be efficiently calculated using equilibrium molecular dynamics (EMD) and grand canonical Monte Carlo (GCMC) simulation techniques. The technical details of such calculations have been extensively discussed elsewhere.^{11,13}

Vishnyakov et al.¹⁰ have recently used GCMC simulations to calculate the adsorption isotherm of CuBTC at 87 K. They found that simple force fields based on the universal force field (UFF)¹⁹ gave results that are in good agreement with their experiments. The atomistic model used in this study is similar to that used by Vishnyakov et al.¹⁰ Briefly, CuBTC is modeled as a rigid framework. Its structure is taken from the literature.^{20,21} The crystal structure of Cui et al.²¹ includes axial oxygen atoms bonded to the

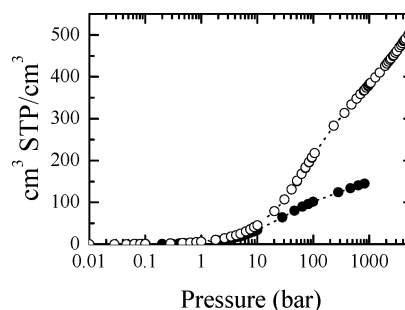


Figure 1. Adsorption of Ar in CuBTC (○) and silicalite (●) at 298 K.

copper, which correspond to water ligands. We simulated dry-CuBTC²¹ with these oxygen atoms removed. Ar was represented as a Lennard-Jones sphere with interactions between pairs of adsorbates and the atoms of the metal–organic framework taken from the literature.²²

Figure 1 shows the adsorption isotherm of Ar in CuBTC at 298 K as compared to the adsorption isotherm of Ar in silicalite, as calculated using GCMC. The details of such simulations have been reported elsewhere.^{11–14} CuBTC has clearly a larger adsorption capacity than silicalite. In these simulations, the infinite dilution isosteric heat of adsorption of Ar in CuBTC was found to be 12.7 kJ/mol. The isosteric heat of adsorption of Ar in silicalite is found experimentally to be 15.8 kJ/mol,²³ while simulations give a value of 12.7 kJ/mol.

To calculate the various diffusivities as a function of the concentration of Ar, we used constant temperature EMD simulations.^{11–14} Previous studies of diffusion of light gases in zeolites^{24,25} have shown that using a rigid lattice is a good approximation for these systems. The structure of MOFs is more open and less dense than that of zeolites, and the extent of their flexibility is as yet unknown. Examples exist of highly stable and rigid MOFs, such as MOF-5¹, and very flexible MOFs, such as Ni₂(4,4'-bipyridine)₃(NO₃)₄.⁷ The simulation of CuBTC as a rigid lattice is an approximation that we believe is accurate for small adsorbents such as Ar at moderate loadings and pressures, although further studies are needed to assess the impact of their flexibility on adsorption and diffusion.

Diffusion in CuBTC, as in zeolites, is found to be an activated process. To compute the activation energy for self-diffusion, we calculated D_s at 200, 298, and 400 K. Figure 2 shows D_s for Ar at infinite dilution, 34 and 80 atoms per unit cell. The resulting activation energies are 6.9, 3.7, and 2.7 kJ/mol, respectively. For comparison, the infinite dilution activation energy of CH₄ in silicalite is found experimentally to be 5.7 kJ/mol,²⁶ while simulations give 4.3 kJ/mol. Thus, the activation energy for diffusion in MOFs is similar to that in silica zeolites.¹⁴

The self-, corrected, and transport diffusivities are all shown in Figure 3 as a function of Ar concentration in CuBTC. In Figure 3,

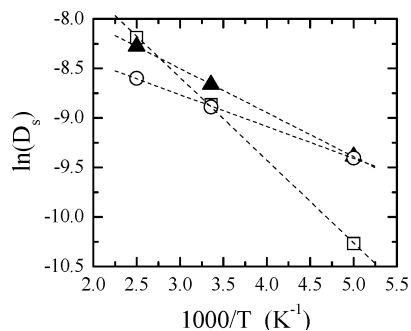


Figure 2. Arrhenius plot of D_s for Ar in CuBTC for infinite dilution (\square), 34 (\blacktriangle), and 80 (\circ) atoms per unit cell, at 200, 298, and 400 K.

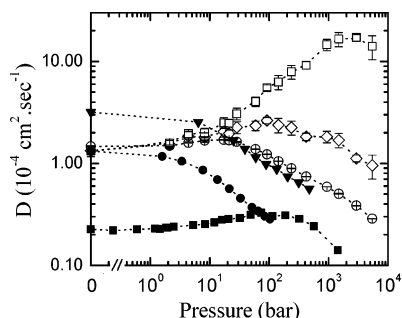


Figure 3. D_s (\circ), D_0 (\diamond), and D_t (\square) of Ar in CuBTC at 298 K. D_s for Ar in silicalite (\bullet), ITQ-7 (\blacktriangledown), and ITQ-3 (\blacksquare) at 298 K. The dotted curves are to guide the eye.

we also show D_s for Ar in three representative zeolites, silicalite, ITQ-7, and ITQ-3, calculated at 298 K.^{11,13} From Figure 3, it is clear that the diffusion of Ar in CuBTC is similar to diffusion in zeolites in magnitude and concentration dependence.

Vishnyakov et al.¹⁰ observed that the most favorable adsorption sites for Ar in CuBTC are in tetrahedral side pockets connected with small windows to the main pores. In our model, the adsorption energy in these pockets is -15.9 kJ/mol, while the adsorption energy in the main pores is -9.2 kJ/mol. We found that Ar could diffuse in and out of these pockets with ease. In fact, from the potential energy surface, it was determined that the barrier for diffusion out of these pockets is 10 kJ/mol. Diffusion barriers of the same magnitude have been observed for Ar and CH₄ in ITQ-3.¹¹ This barrier of 10 kJ/mol for diffusion out of the favorable adsorption sites is larger than the net activation energy of 6.9 kJ/mol seen at infinite dilution. Examination of the trajectories and energy profiles of individual Ar atoms led us to propose the following mechanism for Ar diffusion in CuBTC: For long-range diffusion, Ar can diffuse through the side pockets only, through the main pores only, or through a combination of these two pathways. The energy barrier for diffusion through the main pores only was found to be 3.3 kJ/mol. At low concentrations, Ar can diffuse through all different pathways, leading to the activation energy of 6.9 kJ/mol, a weighted average of all barriers. At higher concentrations, the pathway through the pockets is increasingly less favorable because the side pockets saturate faster.¹⁰ This leads to a lower activation energy for diffusion (see Figure 2). Lower activation energies lead to increasing D_s and D_0 (see Figure 3). At even higher loadings, steric hindrance effects cause a lowering of the diffusivities. Because D_0 is a collective property, the steric hindrance effects are less severe and the maximum is observed at

higher loadings. D_t is the product of D_0 and Γ . Γ is a strongly increasing function of the concentration^{11,13} especially close to saturation. The maximum observed in the transport diffusivity is the arithmetic result of D_0 decreasing faster than Γ is increasing. This has also been observed in zeolites.^{11,13}

In conclusion, our results indicate that diffusion of Ar in CuBTC is very similar to diffusion in silica zeolites in magnitude, concentration, and temperature dependence. Although their chemical composition is rather different, these materials share a structural likeness, as reflected in their crystallographic elements (pore dimensions, channel topologies, and lengths), and an energetic resemblance, manifested in the isosteric heats, diffusion activation energies, and diffusion barriers. The similarity in the diffusional behavior observed for Ar arises from structural and energetic likeness, and it is expected to also hold for other physisorbed species. Given the structural and chemical relationship of CuBTC with other MOFs,^{1–3} this conclusion is expected to apply to a broad range of metal–organic frameworks.

Supporting Information Available: Methodology, description of simulation procedures, and potential landscape data (PDF). This material is available free of charge via the Internet at <http://pubs.acs.org>.

References

- (1) Eddaoudi, M.; Li, H. L.; Yaghi, O. M. *J. Am. Chem. Soc.* **2000**, *122*, 1391–1397.
- (2) Eddaoudi, M.; Moler, D. B.; Li, H. L.; Chen, B. L.; Reineke, T. M.; O'Keefe, M.; Yaghi, O. M. *Acc. Chem. Res.* **2001**, *34*, 319–330.
- (3) Yaghi, O. M.; O'Keefe, M.; Ockwig, N. W.; Chae, H. K.; Eddaoudi, M.; Kim, J. *Nature* **2003**, *423*, 705–714.
- (4) Kärger, J.; Ruthven, D. *Diffusion in Zeolites and Other Microporous Materials*; John Wiley & Sons: New York, 1992.
- (5) Seki, K.; Mori, W. *J. Phys. Chem. B* **2002**, *106*, 1380–1385.
- (6) Pan, L.; Liu, H. M.; Lei, X. G.; Huang, X. Y.; Olson, D. H.; Turro, N. J.; Li, J. *Angew. Chem., Int. Ed.* **2003**, *42*, 542.
- (7) Fletcher, A. J.; Cussen, E. J.; Prior, T. J.; Rosseinsky, M. J.; Kepert, C. J.; Thomas, K. M. *J. Am. Chem. Soc.* **2001**, *123*, 10001–10011.
- (8) Wang, Q. M.; Shen, D. M.; Bulow, M.; Lau, M. L.; Deng, S. G.; Fitch, F. R.; Lemcoff, N. O.; Semancin, J. *Microporous Mesoporous Mater.* **2002**, *55*, p217.
- (9) Eddaoudi, M.; Kim, J.; Rosi, N.; Vodak, D.; Wachter, J.; O'Keefe, M.; Yaghi, O. M. *Science* **2002**, *295*, 469–472.
- (10) Vishnyakov, A.; Ravikovitch, P. I.; Neimark, A. V.; Bulow, M.; Wang, Q. M. *Nano Lett.* **2003**, *3*, 713–718.
- (11) Skoulidas, A. I.; Sholl, D. S. *J. Phys. Chem. B* **2003**, *107*, 10132–10141.
- (12) Skoulidas, A. I.; Sholl, D. S. *J. Phys. Chem. B* **2001**, *105*, 3151–3154.
- (13) Skoulidas, A. I.; Sholl, D. S. *J. Phys. Chem. B* **2002**, *106*, 5058–5067.
- (14) Bowen, T. C.; Falconer, J. L.; Noble, R. D.; Skoulidas, A. I.; Sholl, D. S. *Ind. Eng. Chem. Res.* **2002**, *41*, 1641–1650.
- (15) Theodorou, D. N.; Snurr, R. Q.; Bell, A. T. *Molecular Dynamics and Diffusion in Microporous Materials*. In *Comprehensive Supramolecular Chemistry*; Alberti, G., Bein, T., Eds.; Pergamon Press: New York, 1996; Vol. 7, pp 507–548.
- (16) Keil, F. J.; Krishna, R.; Coppens, M. O. *Rev. Chem. Eng.* **2000**, *16*, 71–197.
- (17) Reyes, S. C.; Sinfelt, J. H.; DeMartin, G. J. *J. Phys. Chem. B* **2000**, *104*, 5750–5761.
- (18) Auerbach, S. M. *Int. Rev. Phys. Chem.* **2000**, *19*, 155–198.
- (19) Rappé, A. K.; Casewit, C. J.; Colwell, K. S.; Goddard, W. A., III; Skiff, W. M. *J. Am. Chem. Soc.* **1992**, *114*, 10024–10035.
- (20) CuBTC crystallizes in the cubic form (*Fm3m*) with a unit cell dimension of 26.343 Å. The main pores of CuBTC have a diameter of 9 Å. It also contains tetrahedral pockets 5 Å in diameter.
- (21) Chui, S. S. Y.; Lo, S. M. F.; Charmant, J. P. H.; Orpen, A. G.; Williams, I. D. *Science* **1999**, *283*, 1148–1150.
- (22) Potential parameters for the Ar–framework interaction were taken from UFF.¹⁹ The parameters for the Ar–Ar interaction were taken from Vishnyakov et al.¹⁰
- (23) Dunne, J. A.; Mariwals, R.; Rao, M.; Sircar, S.; Gorte, R. J.; Myers, A. L. *Langmuir* **1996**, *12*, 5888–5895.
- (24) Demontis, P.; Fois, E. S.; Suffritti, G. B.; Quartieri, S. *J. Phys. Chem.* **1990**, *94*, 4329–4334.
- (25) June, R. L.; Bell, A. T.; Theodorou, D. N. *J. Phys. Chem.* **1990**, *94*, 8232–8240.
- (26) Talu, O.; Sun, M. S.; Shah, D. B. *AIChE J.* **1998**, *44*, 681–694.

JA039215+